Published online 7 July 2007

Nucleic Acids Research, 2007, Vol. 35, No. 14 ***4779–4791***
doi:10.1093/nar/gkm506

Binding parameters and thermodynamics of the interaction of the human cytomegalovirus DNA polymerase accessory protein, UL44, with DNA: implications for the processivity mechanism

Arianna Loregian[1,*], Elisa Sinigalia[1], Beatrice Mercorelli[1], Giorgio Palù[1] and Donald M. Coen[2]

[1]Department of Histology, Microbiology and Medical Biotechnologies, University of Padova, 35121 Padova, Italy and [2]Department of Biological Chemistry and Molecular Pharmacology, Harvard Medical School, Boston, MA 02115, USA

Received April 2, 2007; Revised June 6, 2007; Accepted June 11, 2007

ABSTRACT

The mechanisms of processivity factors of herpesvirus DNA polymerases remain poorly understood. The proposed processivity factor for human cytomegalovirus DNA polymerase is a DNA-binding protein, UL44. Previous findings, including the crystal structure of UL44, have led to the hypothesis that UL44 binds DNA as a dimer via lysine residues. To understand how UL44 interacts with DNA, we used filter-binding and electrophoretic mobility shift assays and isothermal titration calorimetry (ITC) analysis of binding to oligonucleotides. UL44 bound directly to double-stranded DNA as short as 12 bp, with apparent dissociation constants in the nanomolar range for DNAs >18 bp, suggesting a minimum DNA length for UL44 interaction. UL44 also bound single-stranded DNA, albeit with lower affinity, and for either single- or double-stranded DNA, there was no apparent sequence specificity. ITC analysis revealed that UL44 binds to duplex DNA as a dimer. Binding was endothermic, indicating an entropically driven process, likely due to release of bound ions. Consistent with this hypothesis, analysis of the relationship between binding and ionic strength indicated that, on average, 4 ± 1 monovalent ions are released in the interaction of each monomer of UL44 with DNA. The results taken together reveal interesting implications for how UL44 may mediate processivity.

INTRODUCTION

Replicative DNA polymerases are multiprotein complexes that are capable of synthesizing long stretches of DNA. The high processivity of these polymerases is dependent upon accessory proteins called processivity factors that bind to the catalytic subunit of the polymerase and prevent its dissociation from the template. The best-characterized processivity factors are the so-called 'sliding clamps', such as proliferating cell nuclear antigen (PCNA) of eukaryotic DNA polymerases δ and ε (1,2). Sliding clamps possess no inherent DNA-binding capacity, but require clamp-loading proteins to be assembled onto DNA as toroidal homomultimers in an ATP-dependent process (3). After they are loaded onto DNA, the sliding clamps can slide freely along DNA and tether the catalytic subunit to the template, thus ensuring processivity without impeding the movement of the polymerase.

The processivity factors of herpesvirus DNA polymerases employ mechanisms that have yet to be completely explained. The most-studied herpesvirus processivity factor is that of herpes simplex virus (HSV), UL42, which together with the catalytic subunit (UL30) composes the viral DNA polymerase. UL42 differs from sliding clamps in that it binds directly to DNA as a monomer with high affinity and in a manner that does not require clamp loaders or ATP hydrolysis (4–8). Despite the high affinity for DNA, UL42 can diffuse linearly along DNA in the absence of UL30 (9). It has been proposed that electrostatic interactions between basic residues on the α-helical 'back' face of the UL42 structure and the phosphate backbone of DNA (10) provide a tether that

*To whom correspondence should be addressed. Tel: +39 049 8272363; Fax: +39 049 8272355; Email: arianna.loregian@unipd.it
Correspondence may also be addressed to Donald M. Coen. Tel: +1 617 432 1691; Fax: +1 617 432 3833; Email: Don_Coen@hms.harvard.edu

The authors wish it to be known that, in their opinion, the first two authors should be regarded as joint First Authors

prevents dissociation, but allows UL42 to diffuse along the helical backbone. In support of this idea, it has been recently shown that substitutions of arginine residues on the basic surface of UL42 decrease the DNA-binding affinity of the protein (11).

The human cytomegalovirus (HCMV) DNA polymerase is also composed of a catalytic subunit, Pol or UL54, which possesses basal DNA polymerase activity (12,13), and an accessory protein, UL44 (14). UL44 is believed to serve as the processivity factor for the polymerase, as it has been shown to specifically interact with UL54 and to stimulate long-chain DNA synthesis by UL54 (14,15). The crystal structure of residues 1–290 of UL44 (UL44ΔC290) (16) revealed that UL44 has a fold remarkably similar to that of HSV UL42 (10) and monomers of PCNA (1,2), even though these proteins have no obvious sequence homology. In addition, like HSV UL42, HCMV UL44 possesses a basic, α-helical back face, which may be involved in binding to and diffusion along the DNA backbone via electrostatic interactions. However, in contrast to UL42, which is a monomer (4,10,17–19), and PCNA, which is a head-to-tail toroidal homotrimer (1,2), UL44 forms a dimer in solution in the absence of DNA and its crystal structure shows a head-to-head C clamp-shaped homodimer (16,20). Although it has been shown that UL44 can bind double-stranded (ds) DNA and that mutations which affect dimerization also affect DNA binding (15,16,21), the details of the UL44–DNA interaction, including whether UL44 binds DNA as a dimer, have not been yet investigated.

Compared to our knowledge of sequence-specific DNA-binding proteins, derived from numerous structural, biochemical and thermodynamic studies, relatively little is known about how non-sequence-specific DNA-binding proteins interact with DNA. Thus, investigations of proteins such as UL44 can shed light on this class of DNA-binding proteins. In this study, we measured the binding of UL44 to DNA using several techniques, and tested the dependence of binding on various properties of DNA including strandedness, sequence and length. Thermodynamic analysis indicated that UL44 binds DNA as a dimer and that binding is entropically driven, while the dependence of binding on ionic strength allowed an estimation of the number of monovalent ions released in the interaction of UL44 with DNA. The results are consistent with hypothesized electrostatic interactions between basic residues of UL44 and the phosphate backbone of DNA.

MATERIALS AND METHODS

Proteins

The wild-type UL44ΔC290 and mutant UL44ΔC290 L86A/L87A proteins were expressed in and purified from *Escherichia coli* BL21(DE3)pLysS (Novagen) as described previously (16,22). Baculovirus-expressed, full-length UL44, purified as previously described (23), was generously provided by Howard S. Marsden. The purity of the UL44 preparations used for binding studies was estimated to be >90% as assessed by SDS–PAGE followed by silver-staining of the gel (Figure S1). Concentrations of all proteins were determined using amino acid analysis at the Molecular Biology Core Facility, Dana-Farber Cancer Institute.

Oligonucleotides

Single-stranded (ss) oligonucleotides of varying lengths (8, 10, 12, 15, 18, 30 or 47 nt) and sequence were purchased from Integrated DNA Technologies, Inc. (Coralville, IA, USA) or from MWG-BIOTECH AG (Ebersberg, Germany) as gel-purified products. To generate ds oligonucleotides, equal amounts of complementary strands were mixed in annealing buffer (50 mM NaCl, 10 mM Tris, pH 8.0, 1 mM EDTA), completely denatured at 95°C and annealed by slowly cooling to room temperature. Formation of dsDNA was confirmed on a 20% (for shorter oligonucleotides) or 10% (for longer oligonucleotides) non-denaturing polyacrylamide/0.5× Tris–borate EDTA (TBE) gel. The concentrations were determined via UV spectrometry. Some of the oligonucleotides were used as ssDNA in filter-binding assays. These oligonucleotides were designed to be devoid of intramolecular structure. Additionally, prior to assay, they were heated to 95°C for 5 min, and then quick-cooled on ice. For filter-binding and electrophoretic mobility shift assays (EMSAs), oligonucleotides were radiolabeled with [γ-^{32}P]ATP and T4 polynucleotide kinase and purified as previously described (9).

Filter-binding assays

Filter-binding assays were performed by a modification of the double-filter method previously described (5,16). Briefly, 1 fmol of labeled (~10 000 c.p.m./fmol) ssDNA or dsDNA was incubated at room temperature with various amounts of purified UL44ΔC290 or baculovirus-expressed, full-length UL44 for 10 min in a 10 μl volume in binding buffer containing 20 mM Tris–HCl (pH 7.5), 50 mM NaCl, 4% glycerol, 3 mM $MgCl_2$, 0.5 mM DTT, 0.1 mM EDTA and 40 μg of bovine serum albumin (BSA) per milliliter. At the end of the incubation, samples were applied to a nitrocellulose/DE81 filter stack soaked in binding buffer using a vacuum manifold. The DNA–protein complexes were trapped on the nitrocellulose filter (Schleicher and Schuell, Keene, NH, USA) and the remaining, unbound DNA was trapped on the DE81 filter (Whatman, Dassel, Germany) placed under the nitrocellulose filter. Filters were then washed extensively with binding buffer and dried, and radioactivity was measured by liquid scintillation counting. All data were corrected for background (i.e. radioactivity retained on the filter in the absence of UL44). As the concentration of DNA in these filter-binding assays was less than the apparent dissociation constant (K_d) values, these constants were calculated as being equivalent to the amount of protein at which 50% of the DNA was bound by using saturation isotherm analysis.

Experiments to test the affinity of UL44 for DNA in different ionic environments were conducted as described above, but with binding buffers containing 1 mM

Tris–HCl (pH 7.5), 4% glycerol, 0.5 mM DTT, 0.1 mM EDTA, 40 μg/ml BSA and various concentrations of NaCl, KCl, $NaCH_3CO_2$ or $MgCl_2$.

Electrophoretic mobility shift assays (EMSAs)

EMSA reactions (10 μl) contained 1 nM of [^{32}P]-labeled ds oligonucleotide, 20 mM Tris–HCl (pH 7.5), 50 mM NaCl, 4% glycerol, 3 mM $MgCl_2$, 40 μg/ml BSA, 0.1 mM EDTA, 0.5 mM DTT and increasing concentrations of either wild-type UL44ΔC290 or mutant UL44ΔC290 L86A/L87A or baculovirus-expressed, full-length UL44 protein. Mixtures of protein and DNA were incubated for 10 min at room temperature. Following addition of 1 μl of loading buffer (0.025% bromophenol blue, 0.5× TBE and 10% glycerol), bound and free DNA were resolved by fractionation on either a 4% (for analysis of binding of full-length UL44 to ds 30-bp template), or a 5% (for analysis of binding of wild-type or mutant UL44ΔC290 to ds 30-bp template) or 10% (for analysis of binding of UL44ΔC290 to ds 18-bp template) native polyacrylamide gel in 0.5× TBE. Gels were pre-run for 1 h at 10 mA at 4°C, using the Miniprotean II system (Bio-Rad), and run under the same conditions. DNA was visualized using dried gels to expose a phosphor storage screen and the data were analyzed using the Quantity One program (Bio-Rad). The apparent K_d value was calculated from EMSAs with 18-bp dsDNA using the equation:

$$K_d = \frac{[P][DNA_{total}]}{[DNA_{bound}]} - P$$

where [P] is total protein concentration, $[DNA_{total}]$ is total DNA concentration and $[DNA_{bound}]$ is the concentration of bound DNA (24). For EMSAs with 30-bp dsDNA, the apparent K_d values for each binding event were calculated by applying the two-site model of Senear and Brenowitz (25) using the equations:

$$\theta_0 = \frac{1}{Z}$$

$$\theta_1 = K_1 \cdot \frac{L}{Z}$$

$$\theta_2 = K_2 \cdot \frac{L^2}{Z}$$

where θ_i is the fraction of DNA molecules with i ligands bound, L is the concentration of protein ligand, Z is the binding polynomial equal to $1 + K_1 \cdot L + K_2 \cdot L^2$ and K_1 and K_2 are the equilibrium association constants.

Isothermal titration calorimetry (ITC)

ITC experiments were performed using a VP-ITC MicroCalorimeter (MicroCal Inc., Northampton, MA, USA) with protein (UL44ΔC290) concentrations of 3–6 μM and DNA (ds 18- or 30-bp oligonucleotide) concentrations of 30–60 μM. Immediately before the experiments were performed, the protein was extensively dialyzed against buffer containing 20 mM Tris–HCl (pH 7.5), 50 mM NaCl, 5% glycerol, 3 mM $MgCl_2$, 0.1 mM EDTA and decreasing concentrations of DTT until the concentration of DTT was reduced to 0.5 mM, as higher concentrations would interfere with calorimetric measurements. After annealing of complementary strands, the dsDNA oligomers were dialyzed against the same buffer used to dialyze the protein to avoid heat signals from mixing of nonequivalent buffers. All solutions were carefully degassed before the titrations using equipment provided with the calorimeter. Each titration experiment consisted of 10-μl injections of ds oligonucleotide into the protein-containing sample cell at 25°C with a mixing speed of 270 r.p.m. Heats of dilution were determined by titrating the same ds oligonucleotide into the dialysis buffer and buffer into protein and subtracted from the raw titration data before data analysis. The data were integrated to generate curves in which the areas under the injection peaks were plotted against the ratio of DNA oligomer to protein. Analysis of the data was performed using MicroCal Origin version 5.0 provided by the manufacturer according to the one- and two-binding site models. Changes in the free energy and entropy upon binding were calculated from determined equilibrium parameters using the equation:

$$-RT\ln(K) = \Delta G = \Delta H - T\Delta S$$

where R is the universal gas constant ($1.9872\,calmol^{-1}K^{-1}$), T is the temperature in Kelvin degrees, K is the association constant, ΔG is the change in Gibbs free energy, ΔH is the change in enthalpy and ΔS is the change in entropy (26).

Calculation of charge–charge interactions

Quantitative analysis of the effects of changes in salt concentration on the equilibrium binding constant, K_{obs}, for binding of UL44 to ds 18-bp DNA was performed according to the binding theory of Record *et al.* (27,28). According this theory, when a ligand with Z positive charges (or a protein with Z positive charges in its DNA-binding site) binds to a nucleic acid, some number of phosphates (corresponding to Z) are effectively neutralized. As a result, the condensed counterions which were associated with the Z phosphates are released into solution, as well as the ions which were involved in long-range screening interactions. The theory predicts that, in the presence of a monovalent salt MX, the amount of counterion release in a protein–nucleic acid interaction, and therefore the number of ionic interactions involved, may be determined by measurement of the derivative d log K_{obs}/d log $[M^+]$. In a sufficiently diluted solution of the salt MX, where differential hydration effects can be neglected, and if there are no complications from anion binding by the ligand, the predicted quantitative dependence of K_{obs} on $[M^+]$ is (28):

$$\frac{d\log K_{obs}}{d\log[M^+]} = -Z\psi \qquad \mathbf{1}$$

When the binding reaction occurs in the absence of multivalent cations, ψ is a constant (0.88 for duplex B-form DNA) and log K_{obs} is a linear function of log

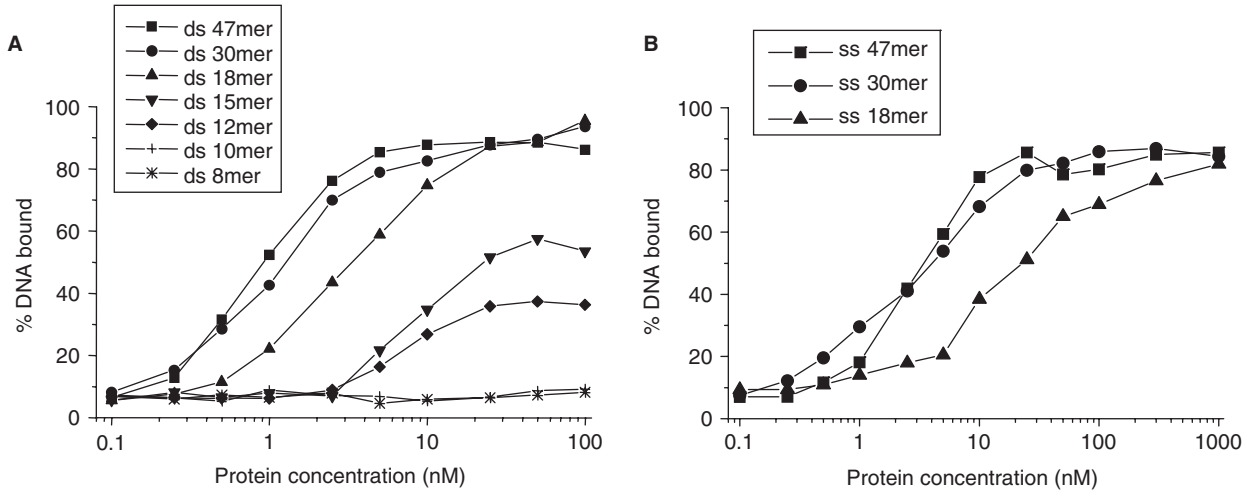

Figure 1. UL44 binding to double-stranded and single-stranded oligonucleotides of different lengths. Increasing concentrations of UL44ΔC290 were incubated with 1 fmol of radiolabeled double-stranded (**A**) or single-stranded (**B**) oligonucleotides (0.1 nM final concentration). Free and protein-bound DNA were quantified by filter-binding assays, and the fraction of protein-bound DNA was plotted against the protein concentration (calculated as a monomer). Apparent dissociation constants correspond to protein concentrations that led to half-maximal occupation of binding sites, as described in legend to Table 1.

$[M^+]$; consequently Z can be determined from the dependence of log K_{obs} on log $[M^+]$.

The effects on K_{obs} caused by divalent ions such as Mg^{2+} are qualitatively similar; however the coefficient ψ in Equation (1) is replaced by φ, which represents the number of divalent counterions thermodynamically associated per phosphate (29):

$$\frac{d \log K_{obs}}{d \log [M^{2+}]} = -Z\varphi \quad \mathbf{2}$$

Therefore, in the absence of preferential anion interactions, the relationship in Equation (3) should hold:

$$\frac{d \log K_{obs}}{d \log [M^{2+}]} = -(\varphi/\psi)\frac{d \log K_{obs}}{d \log [M^{+}]} \quad \mathbf{3}$$

For duplex B-form DNA, $\varphi = 0.47$, and $\varphi/\psi = 0.53$ (29). If Equation (3) does not hold for a particular ligand–nucleic acid interaction, then this suggests that salt effects other than those due to counterion release from the nucleic acid should be considered. In our experiments, Equation (3) did hold.

RESULTS

UL44 binds preferentially to dsDNA with nanomolar affinity and in a sequence-independent manner

To characterize the DNA-binding properties of UL44, we first performed filter-binding assays to determine apparent affinities for ds and ssDNA. Purified UL44ΔC290, a truncated protein that contains the N-terminal 290 residues of UL44 and retains all known biochemical activities of full-length UL44 *in vitro* (21,22) as well as the ability to support origin-dependent DNA replication in transfected cells (A.L. and Pari,G., unpublished data), was used in these assays (this truncated protein will be referred to as UL44 below, unless otherwise specified). Increasing amounts of UL44 were added to 1 fmol of 5′-end-labeled template DNA. A variety of ds and ssDNA oligonucleotides of different lengths and sequence composition were used in these assays. To allow comparison with certain previous measurements of the affinity of HSV UL42 for DNA (5,7), a buffer with relatively low salt concentration (50 mM NaCl) was used in these experiments. The amount of filter-bound radioactivity was measured to determine the fraction of bound DNA, which was plotted against protein concentration (Figure 1). With these experimental conditions, in which the concentration of DNA was very low, we could then apply a saturation isotherm analysis to calculate apparent K_ds from the concentrations of protein that led to half saturation. The K_ds are apparent, rather than absolute because for any length of DNA longer than the size of the binding site for UL44, there are multiple potential binding sites (30,31).

In these assays, UL44 bound dsDNA oligonucleotides with lengths of 18 bp or larger with apparent K_ds in the nanomolar range (Figure 1A and Table 1). With 15- and 12-bp dsDNA templates, the apparent K_ds were markedly higher and UL44 did not bind all of the DNA at the highest concentrations of protein tested, even though binding appeared to plateau (Figure 1A). Possible explanations for this observation are presented in the Discussion section. Detectable binding was observed only with DNAs of at least 12 bp.

Binding titrations with ssDNA templates of 18–47 nt showed that UL44 possesses ~3- to 8-fold greater apparent affinity for dsDNA than for ssDNA of the same length (Figure 1 and Table 1). To test whether the DNA binding of UL44 is affected by the DNA sequence, filter-binding assays were also performed with several sets of ds and ss oligonucleotides of identical length but

Table 1. Apparent dissociation constants of binding of UL44ΔC290 to double-stranded and single-stranded oligonucleotides of different lengths

Oligonucleotide length (bp or nt)	Apparent K_d (nM)[a]	
	ds oligonucleotide	ss oligonucleotide
47	0.9 ± 0.3	3.5 ± 1.2
30	1.2 ± 0.6	4.0 ± 1.6
18	3.1 ± 1.1	23.5 ± 9.8
15	22.3 ± 8.4	–
12	>100	–
10	n.d.	–
8	n.d.	–

[a]Apparent dissociation constants (K_d) were determined from data such as those presented in Figure 1. Apparent K_d = [P][D]/[PD], where apparent K_d is the apparent dissociation constant and [P], [D], and [PD] are the concentrations of free protein, free DNA and the protein–DNA complex, respectively. Since the filter-binding assays were performed under conditions in which $[D] \ll K_d$, apparent dissociation constants correspond to protein concentrations that led to half-maximal occupation of binding sites (i.e. apparent K_d = [P] = $K_{1/2}$). Values are the means of three to five determinations ± SD. n.d.: not detectable. –: not determined.

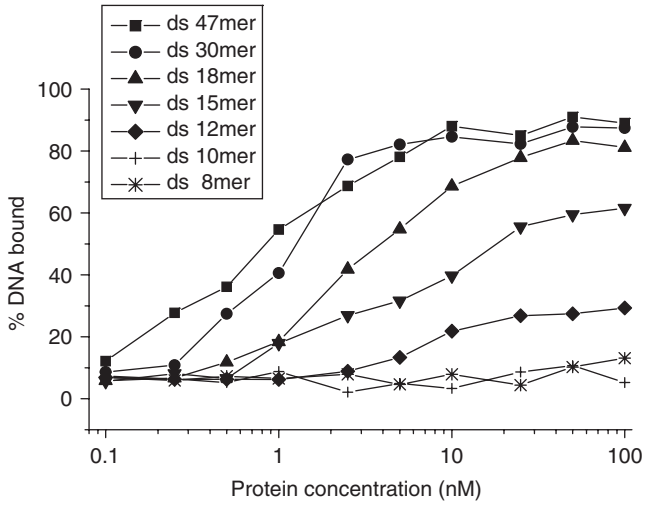

Figure 2. DNA-binding activity of baculovirus-expressed full-length UL44. Reactions were performed as in Figure 1, but contained increasing concentrations of baculovirus-expressed, full-length UL44 protein. Apparent dissociation constants, which correspond to protein concentrations that led to half-maximal occupation of binding sites, are reported in Table 2.

different sequence. Similar apparent K_d values were measured with DNA templates of the same length, regardless of sequence (Table S1). Thus, DNA binding by UL44 is not meaningfully influenced by DNA sequence.

We also investigated whether the C-terminal one-third of UL44 influences DNA binding by performing filter-binding assays with full-length UL44 purified from insect cells infected with a recombinant baculovirus (23). This preparation exhibited an apparent affinity both for dsDNA (Figure 2 and Table 2) and for ssDNA (data not shown) comparable to that of the *E. coli*-expressed, truncated UL44ΔC290 protein, suggesting that the DNA-binding properties of UL44 fully reside in the N-terminal two-thirds of the protein.

Table 2. Apparent dissociation constants of binding of baculovirus-expressed full-length UL44 for double-stranded oligonucleotides of different lengths

Oligonucleotide length (bp)	Apparent K_d (nM)[a]
47	0.8 ± 0.2
30	1.1 ± 0.4
18	3.7 ± 1.2
15	18.8 ± 10.9
12	>100
10	n.d.
8	n.d.

[a]Apparent dissociation constants were calculated as described in the legend to Table 1 from data such as those reported in Figure 2. n.d.: not detectable. Values are the means of two to five determinations ±SD.

Taken together, these observations indicate that UL44 preferentially binds to dsDNA in non-sequence-specific manner and that the formation of DNA–UL44 complexes does not require the C-terminal one-third of the protein. A length of 12 bp is sufficient for UL44 to bind duplex DNA, albeit weakly.

EMSA analysis of stoichiometry of binding and affinity of UL44 for dsDNA

To assess the stoichiometries with which UL44 binds dsDNA, we performed DNA mobility shift assays with radioactively labeled ds 18mer and 30mer oligonucleotides. Although UL44 was able to bind in filter-binding assays to 12-bp DNA (Figure 1), no binding to DNAs of 12 or 15 bp was detected in EMSAs (data not shown), likely due to the necessity for a slightly longer DNA template (i.e. 18 bp) to ensure sufficient binding stability of the protein–DNA complex during gel electrophoresis. Constant amounts of 5′-end-labeled DNA were titrated with increasing amounts of UL44. After a 10-min incubation, the protein–DNA complexes were resolved on a non-denaturing gel. As shown in Figure 3A, incubation of increasing concentrations of UL44 with [^{32}P]-labeled ds 18mer resulted in increasing formation of a single protein–DNA complex (C1) with reduced electrophoretic mobility relative to DNA incubated in the absence of protein. Incubation of UL44 with [^{32}P]-labeled ds 30mer (Figure 3B) resulted mainly in the formation of two complexes (C1 and C2). With increasing amounts of UL44, the lower mobility complex, C2, predominated. EMSA analysis of binding of baculovirus-expressed, full-length UL44 to [^{32}P]-labeled ds 30mer showed a similar pattern (Figure 3C). Given that UL44 forms a dimer in solution (16,20), that dimerization is important for DNA binding (16) and our ITC analysis (see next section), we interpret these results to mean that the faster- and slower-migrating complexes represent 1:1 and 2:1 stoichiometries, respectively, of dimeric UL44 to the ds 30mer. This interpretation is supported by EMSA analysis of an UL44 mutant (UL44ΔC290 L86A/L87A) that is defective in

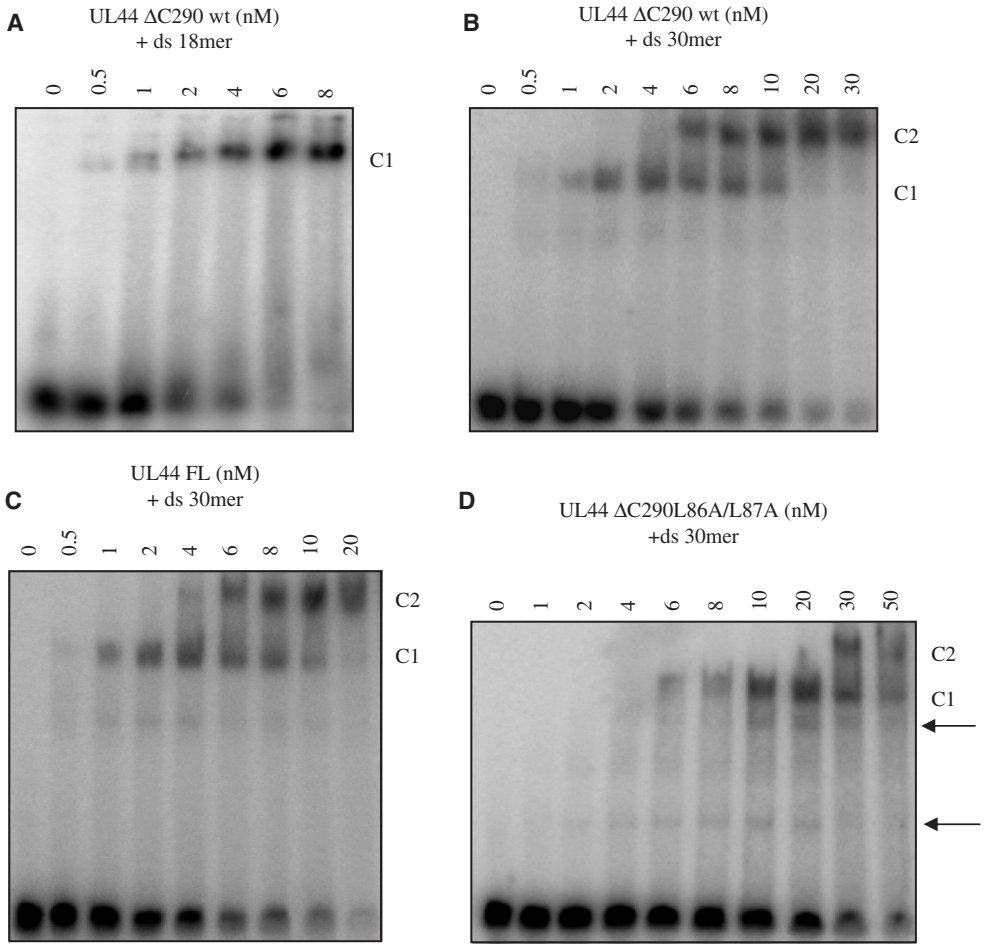

Figure 3. Electrophoretic mobility shift analysis of UL44 binding to double-stranded oligonucleotides. Binding reactions, which contained 1 nM ds 18-bp oligonucleotide and the indicated concentrations of truncated, wild-type (wt) UL44ΔC290 (**A**) or 1 nM ds 30-bp oligonucleotide and truncated, wt UL44ΔC290 (**B**) or full-length, wt UL44 (**C**) or truncated, mutant UL44ΔC290 L86A/L87A protein (**D**), were incubated for 10 min at room temperature in binding buffer prior to separation on a native polyacrylamide gel. The ds templates were formed by annealing synthetic oligonucleotides with their complement. The annealed oligonucleotides were radiolabeled and gel-purified as described in the Materials and Methods section. The arrows in panel D point at faster migrating species, likely corresponding to UL44 monomer–DNA complexes, observed in EMSA analysis of DNA binding of the UL44ΔC290 L86A/L87A mutant, which is defective in dimerization, but not in EMSA with wild-type UL44ΔC290.

dimerization (16) in which faster migrating species are observed, consistent with UL44 monomer–DNA complexes (Figure 3D).

To determine the binding affinity of UL44 for the ds 18mer in these EMSAs, we performed densitometric measurements of free and bound template at different UL44 concentrations. As incubation of this short template at all of the protein concentrations used to calculate affinities resulted in only one complex that migrated more slowly than the unbound template (Figure 3A), the affinities measured reflect one UL44 dimer bound to one DNA molecule. The calculated apparent K_d for the ds 18mer was 2.7 ± 0.9 nM. This value is comparable, within experimental error, with that obtained in filter-binding assays with the same DNA template (Table 1).

We also determined affinities for each of the two binding events on the ds 30mer in these EMSAs from densitometric measurements of free template and the two bound complexes at different UL44 concentrations. In this case, the first binding event had an apparent K_d of 2.1 ± 0.8 nM, while the second had an apparent K_d of 16.2 ± 2.1 nM. Similarly, the apparent K_d of baculovirus-expressed, full-length UL44 was 1.7 ± 0.9 nM for the first binding event and 20.3 ± 6.2 nM for the second. Possible explanations for this difference in affinity are considered in the Discussion section.

ITC analysis of UL44–DNA interactions

We then used ITC to characterize quantitatively the thermodynamics of UL44 binding to dsDNA. ITC measures heat generated or absorbed upon binding (26), and provides in a single experiment the values of the binding constant (K), the stoichiometry and the change of enthalpy (ΔH). The K value then permits calculation of the change in free energy (ΔG), which together the ΔH allows the calculation of the entropic term $T\Delta S$.

We first applied ITC to investigate the energetics of UL44 binding to a ds 18-bp oligonucleotide. Calorimetric titrations were performed in which fixed amounts of

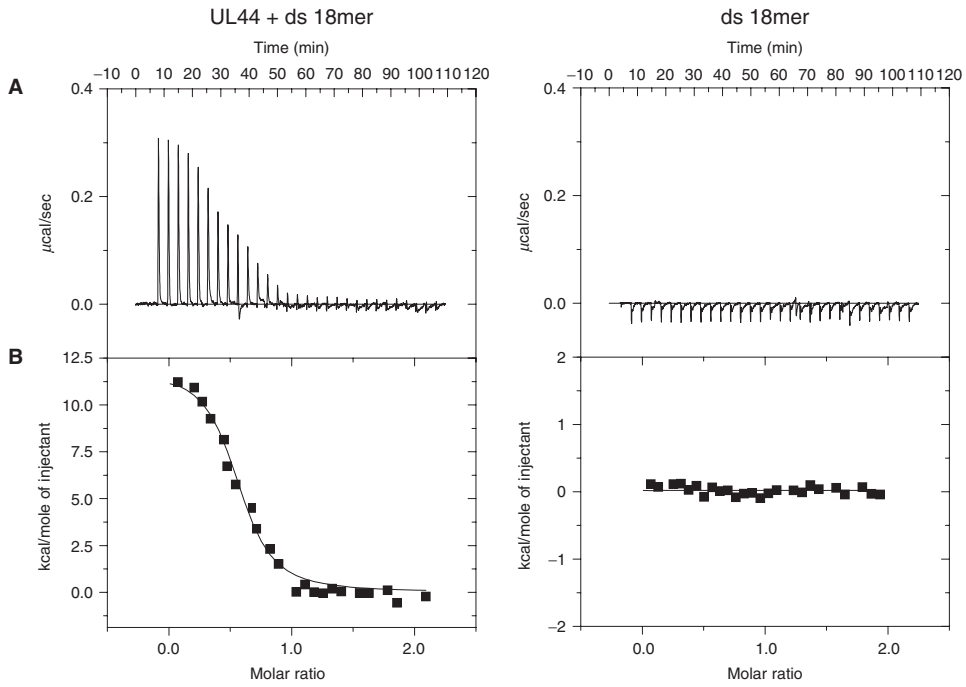

Figure 4. ITC analysis of the binding of UL44 to ds 18-bp DNA. Titrations were performed with 10-µl injections of ds 18mer into a sample cell containing UL44ΔC290 (left panel), or, as a control, buffer only (right panel). (**A**) Raw data for the titrations, in which the power output in microcalories per second is measured as a function of time in minutes. (**B**) The heats of dilution of both protein and DNA were subtracted, and the area under each injection curve was integrated to generate the points, which represent heat exchange in kilocalories per mole and are plotted against the cumulative DNA-to-protein molar ratio for each injection. The solid line represents the best-fit curve for the data. The thermodynamic parameters describing the fit are presented in Table 3.

the 18mer in the syringe were sequentially injected into the sample cell containing purified UL44. The raw data (Figure 4A, left panel) indicate an endothermic interaction, based on the positive values observed for the peaks. With each injection of oligonucleotide, less and less heat uptake was observed until constant values were obtained (corresponding to the heat uptake due to dilution), reflecting a saturable process. Included in Figure 4A (right panel) is a corresponding blank titration in which the DNA was injected in plain buffer (values corresponding to heats of dilution). The heats of dilution of both protein and ligand (DNA) were determined and subtracted prior to analysis, and the data were integrated to generate curves in which the molar ratio of DNA to protein is plotted against the kilocalories per mole of injected DNA. The integrated heats for both titrations are shown in Figure 4B and the parameters for the binding of UL44 to the ds 18-bp oligonucleotide are summarized in Table 3. The analysis shows that the UL44–DNA interaction is characterized by a $K = 3.6 \times 10^8\,\mathrm{M}^{-1}$. This association constant corresponds to an apparent K_d of ~2.8 nM, a value that corresponds closely to those measured in filter-binding assays and EMSAs with the same DNA template. Moreover, the binding of UL44 to the ds 18mer was characterized by a relatively large and positive enthalpy of binding ($+11.0 \pm 0.9$ kcal/mol, Table 3). Very similar results were obtained when UL44 was titrated with ds oligonucleotides of identical length (18 bp) but different sequence (data not shown), confirming the non-sequence-specific nature of UL44–DNA interaction. The positive heat of formation of the UL44–DNA complex indicates that this interaction is an enthalpically unfavorable (entropically driven) process.

The stoichiometry of binding was also determined from our analysis of the calorimetry data. Analysis using a one-site model indicated a stoichiometry of 0.5 DNA mole/protein mole (that corresponds to the molar ratio of DNA to protein at the inflection point of the binding isotherm in Figure 4B, left panel), i.e. one molecule of DNA was bound to two molecules of UL44 polypeptide. Since UL44 forms a dimer in solution (16,20) and as only one UL44–DNA complex was observed with the 18-bp oligonucleotide in EMSA experiments (Figure 3A), the observed stoichiometry of 0.5 further supports the interpretation that UL44 binds this DNA template as a dimer.

To further dissect UL44–DNA binding energetics, calorimetric titrations were performed in which a ds 30-bp oligomer was titrated into UL44. Figure 5A shows the heat effects of 29 subsequent injections of ds 30mer into the sample cell containing UL44 (left panel) or plain buffer (right panel). Binding of UL44 to duplex 30-bp DNA gave rise to a more complex binding isotherm with a curvature typically observed in the presence of multiple, non-equivalent binding sites (Figure 5B, left panel). These additional heat effects at high levels of this DNA were observed repeatedly. Also, in reverse titrations (titrating UL44 into ds 30mer), additional heat effects were observed when DNA was almost completely saturated (data not shown). The biphasic nature of the isotherm suggested two binding sites with markedly different affinities. Indeed, the ITC data were best fit

Table 3. Thermodynamic parameters for binding of UL44 to double-stranded 18-bp DNA

N	K ($\times 10^8\,M^{-1}$)	Apparent K_d ($\times 10^{-9}$ M)	ΔH (kcal/mol)	$T\Delta S$ (kcal/mol)	ΔG (kcal/mol)
0.5 ± 0.1	3.6 ± 0.8	2.8 ± 0.6	11.0 ± 0.9	22.5 ± 1.2	-11.5 ± 0.7

Titrations were performed with 10-µl DNA oligonucleotide injections. Heats of dilution of both oligonucleotide and protein were subtracted from the raw data prior to analysis. Nonlinear least-squares analysis of the raw data was performed with the fitting algorithm provided with the calorimeter. Values are the means of three determinations ± SD.

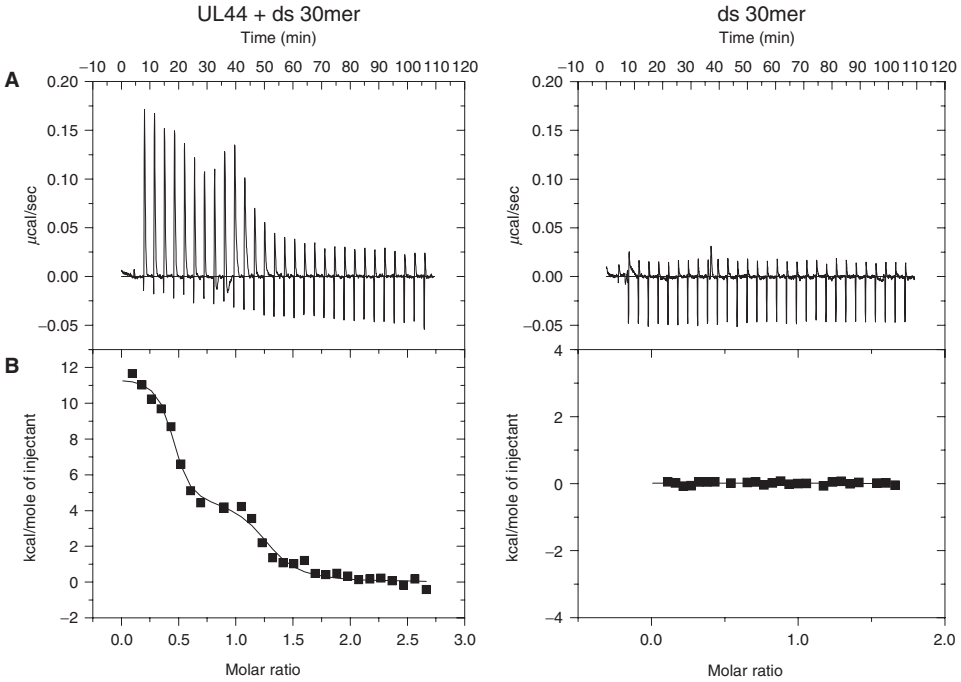

Figure 5. ITC analysis of the binding of UL44 to ds 30-bp DNA. Titrations were performed with 10-µl injections of ds 30mer into a sample cell containing UL44ΔC290 (left panel), or, as a control, buffer only (right panel). (**A**) Raw data for the titrations, in which the power output in microcalories per second is measured as a function of time in minutes. (**B**) The heats of dilution of both protein and DNA were subtracted, and the area under each injection curve was integrated to generate the points, which represent heat exchange in kilocalories per mole and are plotted against the cumulative DNA-to-protein molar ratio for each injection. The solid line represents the best-fit curve for the data. The thermodynamic parameters describing the fit are presented in Table 4.

using a two-site model whose thermodynamic parameters are listed in Table 4. The first site in this model has a higher affinity ($K_1 = 4.1 \times 10^8\,M^{-1}$; apparent $K_d = 2.4$ nM) and larger enthalpy ($\Delta H_1 = 11.8$ kcal/mol). Both values are very similar to those measured in titrations with ds 18-bp DNA (Table 3). The second site exhibits weaker affinity ($K_2 = 1.2 \times 10^7\,M^{-1}$; apparent $K_d = 83$ nM) and a lower enthalpy change ($\Delta H_2 = 4.5$ kcal/mol, Table 4). A possible explanation for these differences in affinity and enthalpy is presented in the Discussion section.

Effect of varying concentrations of mono- and divalent salts on affinity of UL44 for dsDNA

Our results from ITC assays, which showed that binding of UL44 to duplex DNA is entropically driven, suggested that binding may entail the release of bound ions. Similarly, studies of the interaction of various charged protein ligands (e.g. oligolysines, RNAse and *E. coli lac* repressor and RNA polymerase) with nucleic acids have demonstrated that these association reactions are driven by the entropic effect of release of bound cations from the nucleic acid (32). In these cases, the analysis of the ion dependence of equilibrium binding constant, K_{obs}, has allowed investigators to measure the number of participating ions, and has provided information about the molecular details of the binding reaction. In particular, plotting the log K_{obs} versus the log $[M^+]$, where M^+ is a cation, permits the calculation of the number of charge–charge interactions involved in binding.

The dependence of K_{obs} of UL44–DNA interaction on monovalent electrolyte concentration was determined in various buffers, using either Na^+ or K^+ as the cation and either Cl^- or CH_3COO^- as the anion. In every case, log K_{obs} was a linear function of log $[M^+]$, as predicted by Equation (1) (see Materials and Methods section). Figure 6A and B show the results of series of experiments in Tris buffer (1 mM, pH 7.5) using NaCl and $NaCH_3CO_2$, respectively, as the monovalent salt. The least squares slopes d log K_{obs}/d log $[Na^+]$ were -3.53 ± 0.76 and -3.76 ± 0.55, respectively, implying that $\sim 4 \pm 1$ ions are released in the interaction of each monomer of UL44 with dsDNA in the salt range and buffer studied. Then it

Table 4. Thermodynamic parameters for binding of UL44 to double-stranded 30-bp DNA

K_1 ($\times 10^8\,M^{-1}$)	ΔH_1 (kcal/mol)	$T\Delta S_1$ (kcal/mol)	ΔG_1 (kcal/mol)	K_2 ($\times 10^7\,M^{-1}$)	ΔH_2 (kcal/mol)	$T\Delta S_2$ (kcal/mol)	ΔG_2 (kcal/mol)
4.1 ± 0.9	11.8 ± 0.7	23.4 ± 1.1	-11.6 ± 0.8	1.2 ± 0.2	4.5 ± 0.3	14.0 ± 0.6	-9.5 ± 0.9

Titrations were performed with 10-μl DNA oligonucleotide injections. Heats of dilution of both oligonucleotide and protein were subtracted from the raw data prior to analysis. The best fit to the ITC data was obtained by applying a two-site model where K_i, ΔH_i, $T\Delta H_i$ and ΔG_i are the association constant, the enthalpy change, the entropy change and the free energy change, respectively, at the *i*th binding site on the DNA. Values are the means of three determinations ± SD.

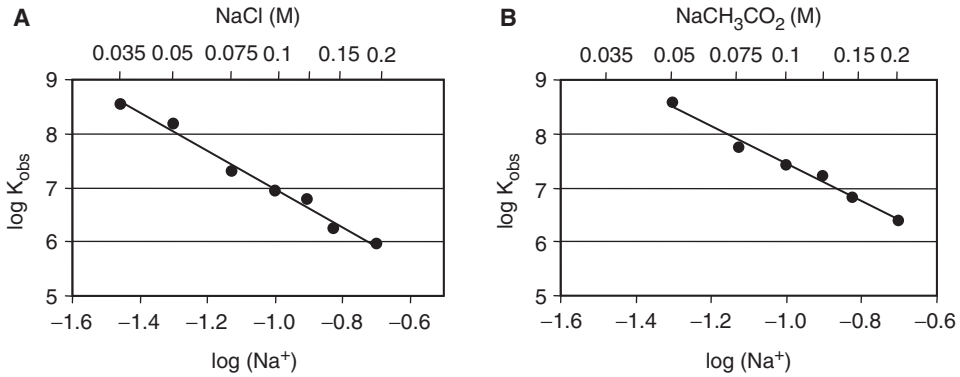

Figure 6. The dependence of the observed binding constant of the UL44–DNA interaction on the concentration of sodium chloride or sodium acetate. Experiments were performed by incubating increasing concentrations of UL44ΔC290 with 1 fmol of radiolabeled ds 18-bp oligonucleotide and in the presence of varying concentrations of sodium chloride (**A**) or sodium acetate (**B**). Free and protein-bound DNA were quantified by filter-binding assays, and, for each salt concentration, a plot such as those shown in Figure 1 was created, wherein the K_d value corresponds to protein concentrations that led to half-maximal occupation of binding sites. The K_{obs} at each salt concentration was calculated as the reciprocal of K_d value. The logarithm of K_{obs} was then plotted as a function of the logarithm of the Na^+ concentration (lower *X*-axis). Salt concentrations used in these experiments are indicated on the upper *X*-axis.

can be estimated (by dividing the least squares slopes by $\psi = 0.88$, the number of Na^+ ions thermodynamically bound per phosphate in dsDNA) that a maximum of 4 ± 1 phosphate groups on the DNA are involved in ionic interactions with positively charged groups on the protein. An additional set of binding data was obtained in the same buffer but with KCl as the variable monovalent salt. Binding constants under these conditions agreed with those in Figure 6A within experimental error (data not shown). Thus, we conclude that the effects of the K^+ and Na^+ ions are similar and that the Tris cation in the buffer has minimal effect on the interaction at the salt concentrations used in the experiments.

If the contribution of anion release to the total observed ion release in the UL44–DNA interaction is small, then *Z*, the number of phosphate groups involved in ionic interactions, corresponds to that estimated from Equation (1). If there is detectable anion release, then *Z* is less than this value. A rather small anion effect on K_{obs} was apparent in a comparison of Figure 6A and B. All conditions in these two sets of experiments were identical, except that in one case the anion was Cl^- and in the other CH_3COO^-. Values of K_{obs} were ~3 times larger in sodium acetate than in sodium chloride at the same Na^+ concentration. In contrast, a 40-fold difference was observed in the non-specific interaction of *E. coli lac* repressor with DNA by replacing Cl^- with CH_3COO^- (29). In any case, the fact that the slopes of the lines in Figure 6A and B differ by only 6% (which is well within the SE of either least-squares line) suggests that there are no major differences in the amount of anion release (if any) in the two systems.

To help remove ambiguities due to anion binding from the determination of *Z*, one can perform protein–nucleic acid binding experiments in the presence of MgX_2 only. This will shift the range of X^- concentrations associated with experimentally accessible values of K_{obs} to substantially lower concentrations, and thereby reduce the importance of anion binding.

The dependence of log K_{obs} of UL44–DNA interaction on log [Mg^{2+}] is shown in Figure 7. The log K_{obs} varied with log [Mg^{2+}] in a linear fashion, within experimental error, as predicted by Equation (2) (see Materials and Methods section) in the absence of monovalent cations and provided that the anion-binding effect is not large. From the slope of the least-squares line in Figure 7 (-1.93 ± 0.42), we conclude that 2 ± 1 divalent ions were released upon formation of the UL44–DNA complex in the presence of $MgCl_2$, consistent with the 4 ± 1 monovalent ions released in sodium chloride. These results are also consistent with our observation of no meaningful anion binding. In this case, the ratio of ion release terms should be 0.53 [see Equation (3) in Materials and Methods section]; the experimental value is ~0.5. We can rule out the possibility of a large number of anion sites with low binding affinities. However, we cannot rule out a small number of anion sites with either low or high affinity. At present, the simplest interpretation of our data is that anion release is not a major factor in the thermodynamics of the reaction.

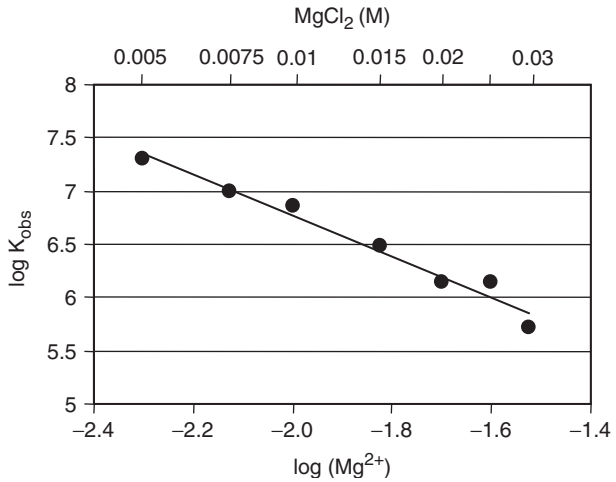

Figure 7. The dependence of the observed binding constant of the UL44–DNA interaction on the concentration of $MgCl_2$. Reactions were performed as in Figure 6, but contained various concentrations of $MgCl_2$. The log K_{obs} was plotted against the log of Mg^{2+} concentration (lower *X*-axis). $MgCl_2$ concentrations used in these experiments are indicated on the upper *X*-axis.

DISCUSSION

Numerous structural and thermodynamic studies have been carried out in recent years in order to characterize the binding of sequence-specific DNA-binding proteins. In contrast, thermodynamic studies of non-sequence-specific DNA-binding proteins have rarely been reported due to the difficulties in studying those systems (33,34). To our knowledge, our studies represent the first investigation of the energetics involved in the interactions of a DNA polymerase accessory protein with DNA. In this study, we used filter-binding experiments under various ionic conditions, EMSAs, and ITC to analyze the interaction of UL44 with several different short DNAs. The combined application of these three techniques sketches a picture of how the HCMV DNA polymerase accessory protein interacts with DNA, and provides some insight into its mechanism of processivity. From a more general point of view, these studies could also contribute to the understanding of the physical principles underlying non-sequence-specific DNA binding.

We will first discuss the stoichiometry of UL44 binding to DNA, the DNA length dependence of this interaction, the importance of electrostatic interactions in UL44–DNA binding and how UL44 compares with other processivity factors. Then, we will discuss how our results could shed some light on the processivity mechanisms of UL44.

UL44 binds to DNA as a dimer

Our data taken together with previous studies (15,16) indicate that UL44, unlike sliding clamp processivity factors, interacts directly with DNA in a manner that does not require ATP hydrolysis or accessory proteins. Previous studies had also shown that UL44 is a dimer in crystals and in solution, and that mutations that affect dimerization reduce DNA binding (16,20). These results suggested, but did not demonstrate that UL44 binds to DNA as a dimer. Here we have shown that UL44 does indeed bind DNA as a dimer. In particular, ITC measurements showed that UL44 bound to a ds 18-bp oligomer with a stoichiometry of 0.5 DNA molecule per UL44 monomer; i.e. one UL44 homodimer per ds 18-bp DNA. Moreover, results from EMSAs are consistent with this conclusion (Figure 3). The ITC data, which fit well with a one-site binding model, further suggest that each monomer within the UL44 dimer contributes equivalent binding energy to the ligand (dsDNA). Although a K_d of ~243 nM has been previously determined for UL44 homodimerization in solution in the absence of DNA (16), in EMSAs we observed formation of UL44 homodimers on DNA at substantially lower protein concentrations (Figure 3). One possible explanation is that binding to DNA effectively increases the concentration of UL44 in one dimension and thereby promotes dimerization. Thus, the K_d value of UL44 homodimerization when bound to DNA could be much lower than the value that has been measured in solution in the absence of DNA.

DNA length dependence of UL44 binding

Experiments with DNAs of varying lengths showed that UL44 binds weakly, but detectably to 12-bp DNA, and undetectably to 10-bp DNA (Figure 1). This suggests a minimum binding length for UL44 binding of 12 bp. This estimate is consistent with modeling studies employing molecular dynamics simulations that place roughly 12 bp of double helix within the UL44 dimer (Komazin,G., Petrella,R., Santos,W.L., Filman,D.J., Hogle,J.M., Verdine,G.L., Karplus,M. and D.M.C. in preparation). UL44 bound more strongly to 15-bp DNA than to 12-bp DNA, and bound with even higher affinity to an 18-bp DNA as a single UL44 dimer. Interestingly, UL44 did not bind all of the 12- and 15-bp DNA, even at high concentrations (Figure 1A). There are several possible mechanisms that could contribute to this failure to saturate. One is that the ends of these short DNAs 'fray' (become ss) in the relatively low salt concentrations used. UL44 binds to ssDNA with lower affinity than to dsDNA, and this difference in affinity increases as length decreases (Figure 1 and Table 1). Perhaps, then, frayed ends on short dsDNAs limit the amount of DNA that can be productively bound. Another possible mechanism is that UL44 so rapidly diffuses off the ends of such short DNAs that this limits productive binding. Such diffusion to DNA ends has been shown previously for HSV UL42 (9,11).

Both EMSAs and ITC assays showed that two UL44 dimers bind to a 30-bp DNA, but that while the first dimer bound with an affinity similar to that observed with an 18-bp DNA, the second dimer bound with a lower affinity. The reduction in affinity between the first and second binding events was ~8-fold in EMSAs and ~35-fold in ITC assays. It is not clear why the two assays would generate different values for the apparent K_d of the second binding event, while yielding similar values for the first event. It is possible that different experimental conditions

or the different models used to analyze the EMSA and ITC data contribute to the different values for the second binding event.

Regardless, the reduction in affinity is not surprising given the DNA length dependence for UL44 binding, as the first UL44 dimer binds to a DNA >18 bp, but when the second dimer binds, there are only 15 bp available to bind each dimer. It is interesting that, unlike the situation where one UL44 dimer was only able to bind a fraction of the 15-bp DNA (Figure 1A), two UL44 dimers could bind essentially all of the 30-bp template, despite each dimer occupying 15 bp (Figure 3). This may be due at least in part to a lack of frayed ends on the longer template or to one UL44 dimer hindering the diffusion of the other UL44 off the DNA. However, it also raises the possibility of dimer–dimer interactions that stabilize the binding of each UL44 on the shorter binding site. More study is required to determine if this is the case; nevertheless, dimer–dimer interactions were observed in one of the crystal structures of UL44 (35). There is a considerable excess of UL44 to UL54 in HCMV-infected cells and it may be that dimer–dimer interactions can occur on viral DNA.

UL44–DNA binding is governed by electrostatic interactions

Examination of the crystal structure of UL44 led to the hypothesis that this protein binds via electrostatic interactions between positively charged lysine residues and the phosphate backbone of DNA (16). Several lines of evidence presented here are in accord with this hypothesis. UL44 exhibited no apparent sequence specificity in binding to DNA, and bound ssDNA with apparent dissociation constants only 3- to 8-fold higher than those for binding dsDNA of the same length. These observations alone suggest that electrostatic interactions between basic residues in UL44 and the phosphate backbone of DNA (rather than other features of DNA) govern binding. This suggestion is further supported by binding being endothermic. This indicates that the interaction is enthalpically unfavorable and, instead, is driven by an increase in entropy. That in turn suggests that the increase in entropy is due to the release of bound ions characteristic of electrostatic interactions. The entropic effect of counterion release into a dilute salt solution has been shown to provide the major contribution to the observed favorable free-energy change driving such non-specific association reactions as the binding of oligolysines, ribonuclease and *E. coli lac* repressor to DNA (28,29,36,37). Finally, further support for electrostatic interactions governing DNA binding by UL44 comes from the observation that the affinity of UL44 for dsDNA decreases with increasing ionic strength and that this is governed by cation release. Thus, all of these findings are consistent with the hypothesis derived from the crystal structure.

Comparisons with HSV UL42 and other DNA polymerase processivity factors

The DNA-binding activity of HCMV UL44 presents several analogies to that of HSV UL42. Like UL42, UL44 directly binds to DNA with relatively high affinity. Indeed, published apparent K_d values for binding of UL42 to ~30-bp DNA range from 1.1 to 3.6 nM (5,7,11), similar to the values we obtained for UL44 under similar ionic conditions. Like UL42, where a ~4000-fold difference in apparent K_d has been reported when potassium chloride is increased from 50 to 125 mM (38), the affinity of UL44 for DNA decreases with increasing ionic strength. As reported here, UL44 binds to ss and dsDNA in a sequence-non-specific manner. Similarly, no sequence specificity has been reported for binding of UL42 to DNA, although this aspect has not been studied in much detail.

However, some interesting differences also emerge from a comparison of the DNA-binding activities of HCMV UL44 and HSV UL42. Although UL44, like UL42, binds dsDNA with higher affinity than ssDNA, the difference in apparent affinity is greater for UL42—~20-fold (5) versus 3- to 8-fold. This difference is likely due to UL42 binding DNA as a monomer (4), via a positively charged face (11), which is relatively flat, at least in the absence of DNA (10), while our data here show that UL44 binds to duplex DNA as a dimer. Thus, binding as a monomer could afford UL42 fewer opportunities for interaction with ssDNA than does the UL44 C clamp dimer.

Several aspects of the UL44–DNA interaction resemble those of PF-8, the processivity factor of human herpesvirus 8 DNA polymerase. Like UL44, PF-8 can form homodimers both in solution and on DNA (20), and PF-8 dimerization has been suggested to be important for binding to DNA (20). Also, similar to UL44, the shortest length of DNA to which PF-8 is able to bind is 14 bp (20). Although this aspect has not yet been investigated quantitatively, we would anticipate that PF-8, like HCMV UL44, but not like HSV UL42, would have only a several-fold higher apparent affinity for ds than for ssDNA. Indeed, DNA-cellulose chromatography experiments showed that the amount of PF-8 eluted from dsDNA is only ~5-fold more than that from ssDNA at the same salt concentration (39).

Some similarities can also be found between UL44 and the processivity factor of mitochondrial DNA polymerase, pol γB. Pol γB, like UL44, possesses intrinsic ability to bind to DNA and has a preference for ds over ssDNA (40). As observed for UL44, pol γB can form homodimers both in solution and when bound to DNA (41,42). However, the DNA-binding sites of UL44 and pol γB dimers likely have different locations in their quaternary structure. In the crystal structure, the C clamp-shaped UL44 homodimer possesses a central cavity that has been suggested to be involved in binding dsDNA (16) and may be analogous to the inner channel of PCNA that surrounds DNA (1,2). In contrast, site-specific deletion mutagenesis identified two surface loops located on opposite sides of the symmetrical pol γB dimer that are required for DNA binding and showed that a single DNA molecule must contact basic residues on both sides of pol γB for stable binding (40,41). The different location of the DNA-binding sites in the two systems could explain why UL44 can bind dsDNAs as short as 12 bp, while for pol γB, binding to DNA has been observed only with dsDNAs of at least 47 bp (40). Like UL44, pol γB binds its

cognate catalytic subunit in the absence of DNA and stimulates its polymerizing activity on activated DNA templates (23,43). However, the DNA-binding activity of pol γB is not required to stimulate the polymerase (40,41). A correlation between the loss of dsDNA-binding activity in UL44 mutant proteins and the loss of stimulation of the cognate catalytic subunit has been reported (15). However, it is not clear whether the effects on DNA binding were specific, since binding of UL44 mutants to UL54 was not assessed. Thus, it has not been rigorously demonstrated that the DNA-binding activity of UL44 is required for stimulation of polymerase. In sum, although pol γB shares some common features with UL44, it is not yet clear whether they utilize similar mechanisms to increase the processivity of their respective Pols.

The finding that UL44 binds DNA as a dimer also suggests interesting comparisons with PCNA. The PCNA homotrimer can bind a wide array of cellular proteins involved in DNA replication, DNA recombination and repair, as well as in cell cycle control (44). Similarly, the UL44 dimer, when bound to DNA and with one monomer bound to UL54, could recruit other viral and/or cellular proteins during viral replication. Indeed, reports from several investigators (14,15,21,22,45–47) and unpublished data from us (E.S. and A.L., unpublished data) suggest that UL44 may interact not only with UL54, but also with several other proteins. Whether these interactions occur or play a role during viral infection remains to be established.

Implications for the processivity mechanism

A key issue for all processivity factors is how to keep the catalytic subunit of the polymerase from dissociating from primer-template without slowing down its translocation. For PCNA and other sliding clamp processivity factors, this issue is resolved by the clamp tethering the catalytic subunit to a ring around the DNA that diffuses freely during translocation. In contrast, herpesvirus processivity factors bind tightly to DNA. In the case of HSV UL42, this does not slow translocation of the DNA (5), evidently because UL42 can diffuse on DNA at a rate as rapid as polymerase translocation (9,11). Although it has not yet been demonstrated, it is likely that UL44, like UL42 and PCNA, can diffuse along the DNA template. As suggested previously for HSV UL42 (9), basic residues of UL44 could be positioned to interact with the negatively charged phosphates on DNA in order to facilitate both a high-affinity interaction and sliding on DNA. Indeed, our analysis of UL44–DNA binding in buffers with various ionic compositions indicates that ~8 cations are released from DNA upon binding of a dimer of UL44. This indicates that ~8 charge–charge interactions between basic residues on the protein and phosphate groups on the DNA are important for UL44–DNA binding. Basic residues on UL44 cluster in two locations—a 'back', α-helical face that includes numerous arginines and lysines (mainly lysines), and a loop from aa 163 to 175 that contains several additional basic residues (both arginines and lysines). This loop is not observed in the crystal structure, but it may extend the UL44 C clamp-shaped dimer around DNA. Thus, UL44 may function as a hybrid processivity factor that wraps around dsDNA (like PCNA) and form favorable electrostatic interactions (like UL42). The number of basic residues per monomer is actually substantially greater than the 4 ± 1 charge–charge interactions per monomer that we have measured here. Moreover, mutational analyses have implicated at least seven basic residues as being important for UL44 binding (Komazin *et al.*, in preparation). The lower number of charge–charge interactions may reflect the number of basic residues per UL44 monomer that, on average, mediate binding or may reflect partial charge–charge interactions contributed by more than one basic residue per DNA phosphate. In either case, phosphates on the DNA may be positioned between basic residues on the DNA permitting ready movement of UL44 in either direction on DNA and thus diffusion, which could permit processivity. Support for such a model could come from a crystal structure of UL44 bound to DNA.

SUPPLEMENTARY DATA

Supplementary Data are available at NAR Online.

ACKNOWLEDGEMENTS

We thank Howard S. Marsden for kindly providing purified baculovirus-expressed UL44, personnel of the Molecular Biology Core Facility, Dana-Farber Cancer Institute for protein quantification and Gloria Komazin, Kevin F. Bryant and Sara Richter for helpful discussions regarding EMSA data analysis. We also gratefully acknowledge Luminita Damian of MicroCal for help with analysis of ITC data. This work was supported by PRIN 2005 (grant no. 2005060941) and MURST EX60% to A.L., and by National Institutes of Health grant AI19838 to D.M.C. Funding to pay the Open Access publication charges for this article was provided by discretionary Coen laboratory funds.

Conflict of interest statement. None declared.

REFERENCES

1. Gulbis,J.M., Kelman,Z., Hurwitz,J., O'Donnell,M. and Kuriyan,J. (1996) Structure of the C-terminal region of p21(WAF1/CIP1) complexed with human PCNA. *Cell*, **87**, 297–306.
2. Krishna,T.S., Kong,X.P., Gary,S., Burgers,P.M. and Kuriyan,J. (1994) Crystal structure of the eukaryotic DNA polymerase processivity factor PCNA. *Cell*, **79**, 1233–1243.
3. Jeruzalmi,D., O'Donnell,M. and Kuriyan,J. (2002) Clamp loaders and sliding clamps. *Curr. Opin. Struct. Biol.*, **12**, 217–224.
4. Randell,J.C. and Coen,D.M. (2004) The herpes simplex virus processivity factor, UL42, binds DNA as a monomer. *J. Mol. Biol.*, **335**, 409–413.
5. Weisshart,K., Chow,C.S. and Coen,D.M. (1999) Herpes simplex virus processivity factor UL42 imparts increased DNA-binding specificity to the viral DNA polymerase and decreased dissociation from primer-template without reducing the elongation rate. *J. Virol.*, **73**, 55–66.
6. Gallo,M.L., Dorsky,D.I., Crumpacker,C.S. and Parris,D.S. (1989) The essential 65-kilodalton DNA-binding protein of herpes simplex

virus stimulates the virus-encoded DNA polymerase. *J. Virol.*, **63**, 5023–5029.
7. Gottlieb,J. and Challberg,M.D. (1994) Interaction of herpes simplex virus type 1 DNA polymerase and the UL42 accessory protein with a model primer template. *J. Virol.*, **68**, 4937–4945.
8. Thornton,K.E., Chaudhuri,M., Monahan,S.J., Grinstead,L.A. and Parris,D.S. (2000) Analysis of in vitro activities of herpes simplex virus type 1 UL42 mutant proteins: correlation with in vivo function. *Virology*, **275**, 373–390.
9. Randell,J.C. and Coen,D.M. (2001) Linear diffusion on DNA despite high-affinity binding by a DNA polymerase processivity factor. *Mol. Cell*, **8**, 911–920.
10. Zuccola,H.J., Filman,D.J., Coen,D.M. and Hogle,J.M. (2000) The crystal structure of an unusual processivity factor, herpes simplex virus UL42, bound to the C terminus of its cognate polymerase. *Mol. Cell*, **5**, 267–278.
11. Randell,J.C., Komazin,G., Jiang,C., Hwang,C.B. and Coen,D.M. (2005) Effects of substitutions of arginine residues on the basic surface of herpes simplex virus UL42 support a role for DNA binding in processive DNA synthesis. *J. Virol.*, **79**, 12025–12034.
12. Cihlar,T., Fuller,M.D. and Cherrington,J.M. (1997) Expression of the catalytic subunit (UL54) and the accessory protein (UL44) of human cytomegalovirus DNA polymerase in a coupled in vitro transcription/translation system. *Protein Expr. Purif.*, **11**, 209–218.
13. Mar,E.C., Patel,P.C. and Huang,E.S. (1981) Human cytomegalovirus-associated DNA polymerase and protein kinase activities. *J. Gen. Virol.*, **57**, 149–156.
14. Ertl,P.F. and Powell,K.L. (1992) Physical and functional interaction of human cytomegalovirus DNA polymerase and its accessory protein (ICP36) expressed in insect cells. *J. Virol.*, **66**, 4126–4133.
15. Weiland,K.L., Oien,N.L., Homa,F. and Wathen,M.W. (1994) Functional analysis of human cytomegalovirus polymerase accessory protein. *Virus Res.*, **34**, 191–206.
16. Appleton,B.A., Loregian,A., Filman,D.J., Coen,D.M. and Hogle,J.M. (2004) The cytomegalovirus DNA polymerase subunit UL44 forms a C clamp-shaped dimer. *Mol. Cell*, **15**, 233–244.
17. Gottlieb,J., Marcy,A.I., Coen,D.M. and Challberg,M.D. (1990) The herpes simplex virus type 1 UL42 gene product: a subunit of DNA polymerase that functions to increase processivity. *J. Virol.*, **64**, 5976–5987.
18. Gallo,M.L., Jackwood,D.H., Murphy,M., Marsden,H.S. and Parris,D.S. (1988) Purification of the herpes simplex virus type 1 65-kilodalton DNA-binding protein: properties of the protein and evidence of its association with the virus-encoded DNA polymerase. *J. Virol.*, **62**, 2874–2883.
19. Crute,J.J. and Lehman,I.R. (1989) Herpes simplex-1 DNA polymerase. Identification of an intrinsic 5′-3′ exonuclease with ribonuclease H activity. *J. Biol. Chem.*, **264**, 19266–19270.
20. Chen,X., Lin,K. and Ricciardi,R.P. (2004) Human Kaposi's sarcoma herpesvirus processivity factor-8 functions as a dimer in DNA synthesis. *J. Biol. Chem.*, **279**, 28375–28386.
21. Loregian,A., Appleton,B.A., Hogle,J.M. and Coen,D.M. (2004) Specific residues in the connector loop of the human cytomegalovirus DNA polymerase accessory protein UL44 are crucial for interaction with the UL54 catalytic subunit. *J. Virol.*, **78**, 9084–9092.
22. Loregian,A., Appleton,B.A., Hogle,J.M. and Coen,D.M. (2004) Residues of human cytomegalovirus DNA polymerase catalytic subunit UL54 that are necessary and sufficient for interaction with the accessory protein UL44. *J. Virol.*, **78**, 158–167.
23. Loregian,A., Rigatti,R., Murphy,M., Schievano,E., Palu,G. and Marsden,H.S. (2003) Inhibition of human cytomegalovirus DNA polymerase by C-terminal peptides from the UL54 subunit. *J. Virol.*, **77**, 8336–8344.
24. Coligan,J.E. (1996) *Current Protocols In Protein Science*. Wiley, Brooklyn, NY, USA.
25. Senear,D.F. and Brenowitz,M. (1991) Determination of binding constants for cooperative site-specific protein-DNA interactions using the gel mobility-shift assay. *J. Biol. Chem.*, **266**, 13661–13671.
26. Wiseman,T., Williston,S., Brandts,J.F. and Lin,L.N. (1989) Rapid measurement of binding constants and heats of binding using a new titration calorimeter. *Anal. Biochem.*, **179**, 131–137.
27. Record,M.T.Jr, Anderson,C.F. and Lohman,T.M. (1978) Thermodynamic analysis of ion effects on the binding and conformational equilibria of proteins and nucleic acids: the roles of ion association or release, screening, and ion effects on water activity. *Q. Rev. Biophys.*, **11**, 103–178.
28. Record,M.T.Jr, Lohman,M.L. and De Haseth,P. (1976) Ion effects on ligand-nucleic acid interactions. *J. Mol. Biol.*, **107**, 145–158.
29. deHaseth,P.L., Lohman,T.M. and Record,M.T.Jr. (1977) Nonspecific interaction of lac repressor with DNA: an association reaction driven by counterion release. *Biochemistry*, **16**, 4783–4790.
30. McGhee,J.D. and von Hippel,P.H. (1974) Theoretical aspects of DNA-protein interactions: co-operative and non-co-operative binding of large ligands to a one-dimensional homogeneous lattice. *J. Mol. Biol.*, **86**, 469–489.
31. Epstein,I.R. (1978) Cooperative and non-cooperative binding of large ligands to a finite one-dimensional lattice. A model for ligand-oligonucleotide interactions. *Biophys. Chem.*, **8**, 327–339.
32. Lohman,T.M. and Mascotti,D.P. (1992) Thermodynamics of ligand-nucleic acid interactions. *Methods Enzymol.*, **212**, 400–424.
33. Lundback,T., Hansson,H., Knapp,S., Ladenstein,R. and Hard,T. (1998) Thermodynamic characterization of non-sequence-specific DNA-binding by the Sso7d protein from Sulfolobus solfataricus. *J. Mol. Biol.*, **276**, 775–786.
34. McAfee,J.G., Edmondson,S.P., Zegar,I. and Shriver,J.W. (1996) Equilibrium DNA binding of Sac7d protein from the hyperthermophile Sulfolobus acidocaldarius: fluorescence and circular dichroism studies. *Biochemistry*, **35**, 4034–4045.
35. Appleton,B.A., Brooks,J., Loregian,A., Filman,D.J., Coen,D.M. and Hogle,J.M. (2006) Crystal structure of the cytomegalovirus DNA Polymerase subunit UL44 in complex with the C terminus from the catalytic subunit: differences in structure and function relative to unliganded UL44. *J. Biol. Chem.*, **281**, 5224–5232.
36. Record,M.T.Jr, deHaseth,P.L. and Lohman,T.M. (1977) Interpretation of monovalent and divalent cation effects on the lac repressor-operator interaction. *Biochemistry*, **16**, 4791–4796.
37. Lohman,T.M., deHaseth,P.L. and Record,M.T.Jr. (1980) Pentalysine-deoxyribonucleic acid interactions: a model for the general effects of ion concentrations on the interactions of proteins with nucleic acids. *Biochemistry*, **19**, 3522–3530.
38. Chaudhuri,M. and Parris,D.S. (2002) Evidence against a simple tethering model for enhancement of herpes simplex virus DNA polymerase processivity by accessory protein UL42. *J. Virol.*, **76**, 10270–10281.
39. Chan,S.R. and Chandran,B. (2000) Characterization of human herpesvirus 8 ORF59 protein (PF-8) and mapping of the processivity and viral DNA polymerase-interacting domains. *J. Virol.*, **74**, 10920–10929.
40. Carrodeguas,J.A., Pinz,K.G. and Bogenhagen,D.F. (2002) DNA binding properties of human pol gammaB. *J. Biol. Chem.*, **277**, 50008–50014.
41. Carrodeguas,J.A., Theis,K., Bogenhagen,D.F. and Kisker,C. (2001) Crystal structure and deletion analysis show that the accessory subunit of mammalian DNA polymerase gamma, Pol gamma B, functions as a homodimer. *Mol. Cell*, **7**, 43–54.
42. Yakubovskaya,E., Chen,Z., Carrodeguas,J.A., Kisker,C. and Bogenhagen,D.F. (2006) Functional human mitochondrial DNA polymerase gamma forms a heterotrimer. *J. Biol. Chem.*, **281**, 374–382.
43. Lim,S.E., Longley,M.J. and Copeland,W.C. (1999) The mitochondrial p55 accessory subunit of human DNA polymerase gamma enhances DNA binding, promotes processive DNA synthesis, and confers N-ethylmaleimide resistance. *J. Biol. Chem.*, **274**, 38197–38203.
44. Maga,G. and Hubscher,U. (2003) Proliferating cell nuclear antigen (PCNA): a dancer with many partners. *J. Cell. Sci.*, **116**, 3051–3060.
45. Krosky,P.M., Baek,M.C., Jahng,W.J., Barrera,I., Harvey,R.J., Biron,K.K., Coen,D.M. and Sethna,P.B. (2003) The human cytomegalovirus UL44 protein is a substrate for the UL97 protein kinase. *J. Virol.*, **77**, 7720–7727.
46. Marschall,M., Freitag,M., Suchy,P., Romaker,D., Kupfer,R., Hanke,M. and Stamminger,T. (2003) The protein kinase pUL97 of human cytomegalovirus interacts with and phosphorylates the DNA polymerase processivity factor pUL44. *Virology*, **311**, 60–71.
47. Prichard,M.N., Lawlor,H., Duke,G.M., Mo,C., Wang,Z., Dixon,M., Kemble,G. and Kern,E.R. (2005) Human cytomegalovirus uracil DNA glycosylase associates with ppUL44 and accelerates the accumulation of viral DNA. *Virol. J.*, **2**, 55.